

# Phase Behavior of a Designed Cyclopropyl Analogue of Monoolein: Implications for Low-Temperature Membrane Protein Crystallization\*\*

Livia Salvati Manni, Alexandru Zabara, Yazmin M. Osornio, Jendrik Schöppe, Alexander Batyuk, Andreas Plückthun, Jay S. Siegel,\* Raffaele Mezzenga,\* and Ehud M. Landau\*

**Abstract:** Lipidic cubic phases (LCPs) are used in areas ranging from membrane biology to biodevices. Because some membrane proteins are notoriously unstable at room temperature, and available LCPs undergo transformation to lamellar phases at low temperatures, development of stable low-temperature LCPs for biophysical studies of membrane proteins is called for. Monodihydrosterculin (MDS) is a designer lipid based on monoolein (MO) with a configurationally restricted cyclopropyl ring replacing the olefin. Small-angle X-ray scattering (SAXS) analyses revealed a phase diagram for MDS lacking the high-temperature, highly curved reverse hexagonal phase typical for MO, and extending the cubic phase boundary to lower temperature, thereby establishing the relationship between lipid molecular structure and mesophase behavior. The use of MDS as a new material for LCP-based membrane protein crystallization at low temperature was demonstrated by crystallizing bacteriorhodopsin at 20°C as well as 4°C.

Lipidic cubic phases (LCPs) act as thermodynamically

stable, structured, and transparent lipid–water gel-like matrices,<sup>[1]</sup> with curved and homogenous aqueous channels, consonant with an array of host–guest functions, including membrane protein incorporation and crystal nucleation for biophysical studies,<sup>[2,3]</sup> drug delivery,<sup>[4]</sup> food emulsification,<sup>[5]</sup> biodevice fabrication,<sup>[6]</sup> and protocell/membrane biology.<sup>[7]</sup> They were proposed as intermediates in membrane fusion events<sup>[8]</sup> and were observed in stressed, diseased, or virally infected cells.<sup>[9]</sup> Significantly, LCPs stand out as the biomaterials par excellence for crystallization of membrane proteins.<sup>[10]</sup>

Bicontinuous LCPs are three-dimensionally ordered molecular systems made up of a geometrically well-defined, curved lipid bilayer, which is surrounded by two non-connected aqueous channels.<sup>[11]</sup> Lipid and water molecules diffuse freely within their respective molecular subsystem, and in the fully hydrated regime water can diffuse between the confined channels of LCPs and an excess reservoir. Variation of hydration, temperature, and pressure affect phase stability and control formation of various phases with defined material properties,<sup>[12]</sup> the most remarkable thereof being thermodynamic and structural stability of LCPs in excess water. This insolubility in water opens up a plethora of possible uses.

The phase behavior of monoolein (MO), the best-studied lipid forming LCPs (Figure 1a), and the structure and properties of its various phases have been well-established.<sup>[13]</sup> Curvature of the channel is a characteristic parameter of lipidic phases, with the highest curvature associated with the high-temperature phases. Placement of the *cis*-double bond in the chain and head group modification, especially charged modifications, are known to influence curvature and hence phase behavior.<sup>[14]</sup> In the field of membrane structural biology, a number of lipids are already available for LCP-induced crystallization. With the deeper understanding obtained from such studies it is envisaged that changing the lipid structure can be used to influence the subtle balance of phases.

Most LCPs used to date are based on naturally or commercially available lipids, mainly monoacylglycerols. Testing of various available monoacylglycerols to optimize crystallization screens of membrane proteins, and to control phase behavior beyond MO, is an important tool that is widely used in crystal screening and optimization.<sup>[15]</sup> Clearly, control of the chemical properties and mesoscopic dimensions within these matrices can empower numerous technological appli-

[\*] L. Salvati Manni,<sup>[1]</sup> Dr. Y. M. Osornio, Prof. Dr. J. S. Siegel, Prof. Dr. E. M. Landau  
Department of Chemistry, University of Zürich  
Winterthurerstrasse 190, 8057 Zürich (Switzerland)  
E-mail: ehud.landau@chem.uzh.ch

Dr. A. Zabara,<sup>[2]</sup> Prof. Dr. R. Mezzenga  
Department of Health Science & Technology, ETH Zürich  
Schmelzbergstrasse 9, 8092 Zürich (Switzerland)  
E-mail: raffaele.mezzenga@hest.ethz.ch

J. Schöppe, Dr. A. Batyuk, Prof. Dr. A. Plückthun  
Department of Biochemistry, University of Zürich  
Winterthurerstrasse 190, 8057 Zürich (Switzerland)  
Prof. Dr. J. S. Siegel  
School of Pharmaceutical Science and Technology  
Tianjin University  
92 Weijin Road, Nankai District, Tianjin, 300072 (PR China)  
E-mail: dean\_spst@tju.edu.cn

[†] These authors contributed equally to this work.

[\*\*] We are grateful to Stephan Handschin for the optical microscope imaging. We also thank Beat Blattmann and Céline Stutz-Ducommun from the Protein Crystallization Center (Department of Biochemistry, University of Zürich) for their continuing and expert support.

Supporting information for this article including purification, crystallization, and structure determination of bacteriorhodopsin is available on the WWW under <http://dx.doi.org/10.1002/anie.201409791>.

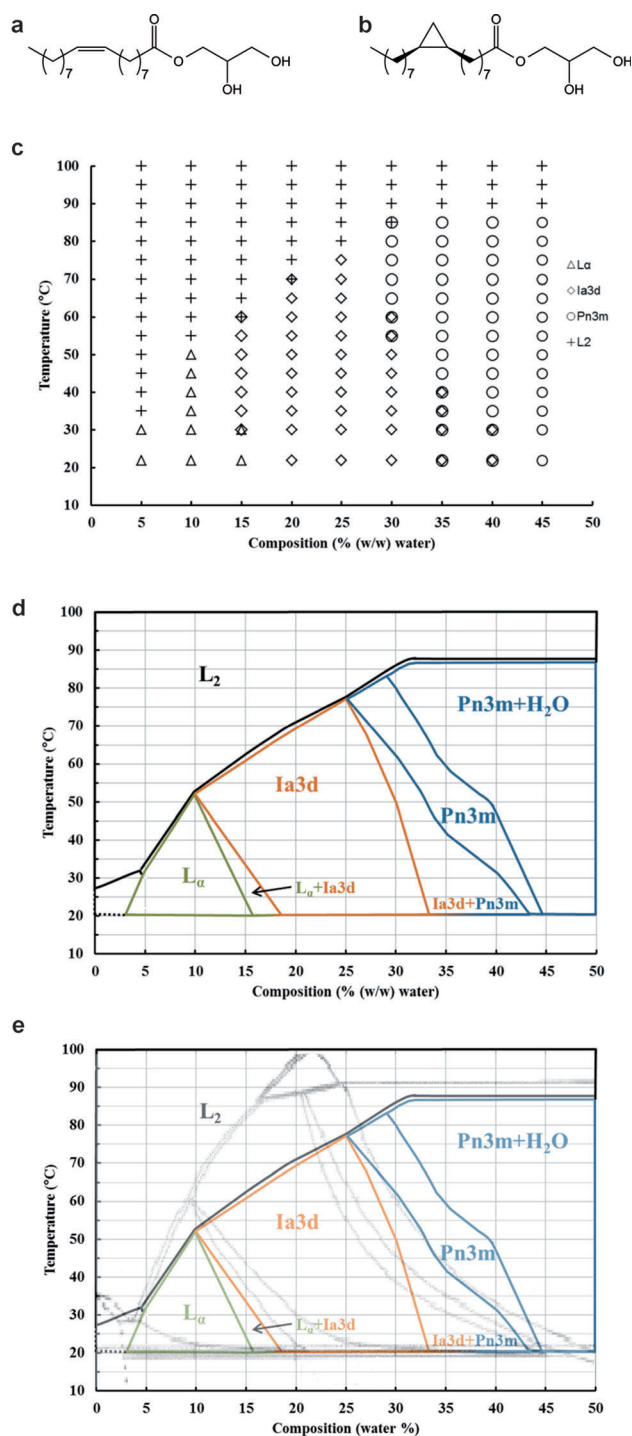


**Figure 1.** Structures of a) monoolein (MO): 1-(*cis*-9-octadecenoyl)-*rac*-glycerol; b) MDS:1-(*cis*-9,10-methylene-octadecanoyl)-*rac*-glycerol. c) Identity and location of each phase (or coexistence of phases) within the composition/temperature space in the MDS:water system, established by SAXS. Phases are: (Δ) L<sub>α</sub>: lamellar phase; (◇) Ia3d: bicontinuous double gyroid cubic phase; (○) Pn3m: bicontinuous double diamond cubic phase; (+) L2: inverse micellar solution. d) Sample composition/temperature phase diagram of the MDS:water system based on interpretation of the data in (c), taking into account evolution of the structural parameters in order to establish the phase maximum hydration, and implicitly coexistence of the bulk phase with excess water. e) Overlay of the binary phase diagrams of MDS (solid lines) and MO (background). The latter was adapted from H. Qiu, M. Caffrey.<sup>[13b]</sup>

cations of LCP; however, to design LCPs with specific structure and phase behavior requires new basic molecular motifs and rigorous phase characterization to elucidate LCP structure/property principles. The discovery reported herein that monodihydrosterculin (MDS), the designer cyclopropyl analogue of monoolein, forms a new, thermodynamically stable low-temperature LCP material directly addresses this goal. Establishment of its extended phase diagram, which differs in a number of fundamental ways from that of MO provides a basis for developing sorely needed design principles in this area.

To date, LCP-generated crystals yielded about 10% of all membrane protein structures. Significantly, most structures of the pharmacologically important family of G protein-coupled receptors (GPCRs), except visual rhodopsin and several stabilized neurotensin receptor variants,<sup>[16]</sup> were determined from LCP-grown crystals. These results were obtained at room temperature. Available LCPs undergo transformation to crystalline lamellar phases at low temperatures.<sup>[13]</sup> This greatly limits the use of LCPs, and calls for the design and development of stable low-temperature LCPs for biochemical and biophysical studies. The reasons for seeking low-temperature LCPs are manifold: Some membrane proteins are notoriously unstable at room temperature,<sup>[17]</sup> requiring low temperature for structural and functional studies. In addition, diffusion is known to be a necessary and crucial process in nucleation and crystal growth: too fast a diffusion may lead to irreversible aggregation and precipitation, while a too slow one may never lead to mature crystals. Having at one's disposal LCPs in a very broad range of temperatures is a clear advantage for controlling diffusion in the lipidic bilayer and in the water channels. Moreover, size of the aqueous channels of the LCPs is an important variable, and the larger the temperature range available, the more flexibility there is in terms of size. Last, recent advances in free electron laser (FEL) science and technology<sup>[18]</sup> offer novel prospects in structural biology. Specifically, the availability of LCP injectors makes it feasible to attempt and crystallize complexes of membrane proteins with other membrane proteins or with soluble proteins, which is at the frontier of membrane structural biology, requiring novel lipidic systems that are thermodynamically stable at low temperature.

Although available LCPs such as the MO-based one can form supercooled systems that can be maintained in the cubic phase to produce low-temperature crystals under certain conditions,<sup>[15]</sup> they do not form thermodynamically stable LCPs at low temperature, and are therefore prone to phase transition. In addition, the handling of minute amounts of LCP is not trivial, and any additional component, such as the various additives needed for membrane protein crystallization, may affect phase stability. The same holds for surface effects, which are very pronounced when setting up small drops (in the nL range). Lipids with cyclopropylated chains occur in several natural systems,<sup>[19]</sup> and their influence on phase transitions, compared to unsaturated chains, has been investigated.<sup>[20]</sup> We therefore sought to design a lipid with alkyl chain length, polarity, and nature of the head group that are similar to those of MO, the most widely used lipid forming LCPs,<sup>[21]</sup> but with increased rigidity of the side chain

compared to conventional *cis* double bond-containing lipids used so far. The target lipid, MDS, contains an identical headgroup to that of MO, and a rigid cyclopropyl moiety replacing the *cis* double bond between C<sub>9</sub> and C<sub>10</sub>, giving rise to a different curvature and different dihedral angles of the hydrophobic tail.

The design of the novel lipid monodihydrosterculin (MDS) implements a geometrically confined cyclopropyl ring as a saturated “*cis*-kink” surrogate (Figure 1b). The resultant LCP phase behavior of MDS supports the use of a small-ring replacement principle, from which other novel LCP lipids can be designed and their properties anticipated.

An additional parameter that could influence phase behavior is the equilibrium composition of esters formed at the 1- and 2-position on the glycerol head group.<sup>[22]</sup> Indeed, hydrated monoacylglycerols undergo spontaneous acyl migration at moderate temperatures, yielding a mixture of about 9:1 of the 1- and 2-isomers.<sup>[23]</sup> This balance seems to be overlooked in previous discussions of MO-LCP and may account for material variability. To ascertain that the data obtained are reproducible with respect to composition all measurements were performed with a pre-equilibrated mixture of (9:1) 1-MDS to 2-MDS (see the Materials and Methods section in the Supporting Information).

The binary MDS:H<sub>2</sub>O phase diagram, established by small-angle X-ray scattering (SAXS) and melting point determination features order-to-order transitions from the *L*<sub>α</sub> to *Ia3d*, and from *Ia3d* to *Pn3m* upon hydration, and formation of the fully hydrated *Pn3m* cubic phase above a characteristic boundary of full hydration (Figure 1c,d). At high temperature, all phases transform into the isotropic L<sub>2</sub> phase. The sequence of transitions is the same as that of MO, but the resulting phase behavior is different because of the stability of each phase. Significantly, the high-temperature H<sub>II</sub> phase that appears in other monoacylglycerol systems<sup>[13]</sup> is absent in the new system. The highly curved H<sub>II</sub> phase has the highest packing frustration energy, and its absence may be correlated with a difference in the chain stretching energy because of the new hydrophobic motif.<sup>[24]</sup>

Overlay of the binary phase diagrams of MDS and MO (Figure 1e) reveals that at a given composition, the collapsing temperature of any phase to the high-temperature L<sub>2</sub> phase is lower in the MDS than in the MO system. The boundary lines between L<sub>2</sub> and the lower-temperature phases in these two systems are not parallel, and form a wedge that broadens with increasing hydration: at low water content (5%) the transition from *L*<sub>α</sub> to L<sub>2</sub> is isothermal (35°C) in both systems. Upon increasing the water content the MDS mesophases become increasingly less stable at high temperature, which is reflected in a relatively low collapsing temperature: thus at 15% water the *Ia3d* to L<sub>2</sub> transition temperatures are 65 and 85°C for the MDS and MO systems, respectively.

The cubic-*Ia3d* is the most pronounced phase in both MO and MDS phase diagrams. For MDS, the *L*<sub>α</sub>-*Ia3d* boundary is at lower water content than in MO, whereas the *Ia3d*-*Pn3m* boundary starts at lower hydration at low temperature, and ends at higher hydration at high temperature (Figure 1e). At even higher water content, the fully hydrated *Pn3m* phase is shifted to higher water content in MDS. Thus, the existence of

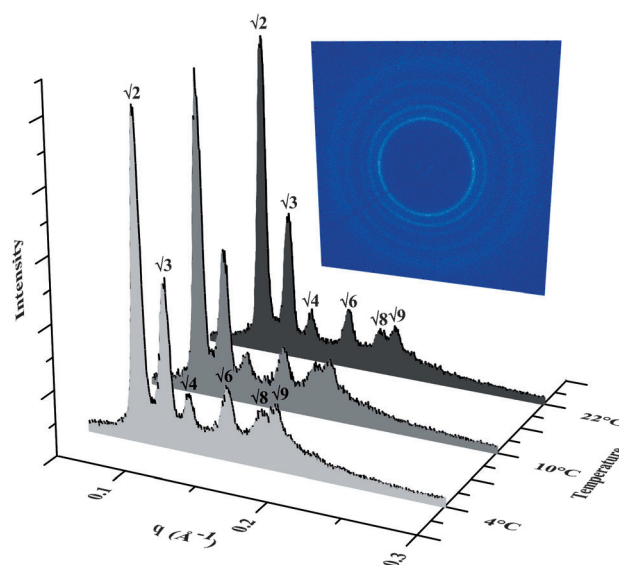


**Figure 2.** 1D SAXS spectra of the scattered intensities versus scattering vector  $q$ , depicting the diffraction patterns of MDS mesophases containing 50% (w/w) water at the selected temperatures. The double diamond *Pn3m* cubic phase exists in the temperature range of 4–22°C, as revealed by the SAXS diffraction peaks in the ratio:  $\sqrt{2}:\sqrt{3}:\sqrt{4}:\sqrt{6}:\sqrt{8}:\sqrt{9}$ .

the cubic phase for MDS is larger in the composition space, and smaller in the temperature space when compared to MO.

Significantly, MDS exhibits a thermodynamically stable cubic phase at low temperature (Figure 2). This observation is in accord with the finding that the high-temperature boundaries of MDS phases are lower than those of MO. Currently available LCPs are often limited in the range of temperature over which they can be used, and are generally unstable at low temperatures (0–4°C), undergoing phase transition into a crystalline phase.<sup>[13]</sup> Therefore, formation of a stable cubic phase at low temperature would have significant implications in biomaterial science and technology in general, and in membrane structural biology in particular.

For a given phase at constant temperature, an increase in water content results in an increase of the lattice size (Figure 3). For the lamellar phase, this corresponds to the inter-bilayer distance, that is, thickness of the aqueous compartment. For the cubic phases, this corresponds to the aqueous channel size. At a given temperature there is a maximal hydration for a certain phase, above which coexistence with a higher hydrated phase sets in. The coexistence region eventually transforms into the pure higher hydrated phase upon further increase of water (Figure 3). In the coexistence regime, the lattice parameter remains constant until complete phase transition is accomplished (Figure 3b and Figure S3 in the Supporting Information). The curvature and the size variation of the unit cell are phase-dependent: The *L*<sub>α</sub> and the cubic *Pn3m* have smaller lattice parameters and the cubic *Ia3d* has larger lattice parameters (Figure 3b, Figure S3).

The phase diagram of the MDS:H<sub>2</sub>O system (Figure 1) demonstrates a number of novel features that can be directly related to the molecular geometry of the hydrophobic chain,

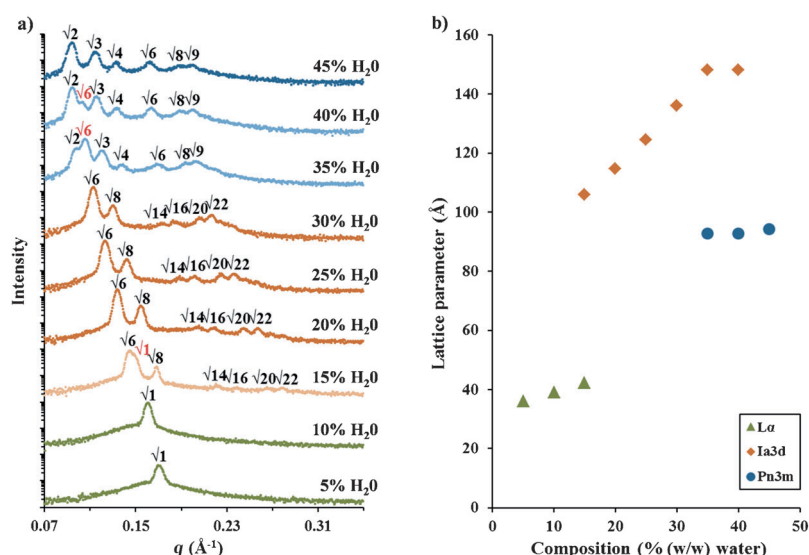


**Figure 3.** a) SAXS spectra of the scattered intensities versus scattering vector  $q$ , azimuthally averaged into 1D profiles, showing the structural evolution of the MDS:water system with increasing hydration at a constant temperature (30 °C). The spectra reveal a series of order to order transitions with the following phase sequence:  $L_{\alpha}$  (green)  $\rightarrow$   $L_{\alpha} + Ia3d$  (beige)  $\rightarrow$   $Ia3d$  (red)  $\rightarrow$   $Ia3d + Pn3m$  (pale blue)  $\rightarrow$   $Pn3m$  (blue), each phase being unequivocally characterized because of its unique diffraction peak ratios. b) Evolution of the lattice parameter size as a function of hydration for the different mesophases in the MDS:water system at 30 °C.

and its packing arrangement within various mesophases. As can be seen from the broader existence range of the cubic phases, the MDS system can accommodate more molecules of water in the cubic phase. Most importantly, this system, which possesses a rigid and more restricted cyclopropyl geometry, was shown to form curved cubic phases at lower temperature than the corresponding MO system, analogous to observed differences between corresponding phosphatidylethanolamines.<sup>[19]</sup> As a consequence, the high-temperature, highly curved reverse hexagonal phase, which appears in most known hydrated monoacylglycerol systems, is absent in the phase diagram of MDS. Moreover, the MDS system forms a stable  $Pn3m$  cubic phase at 4 °C (Figure 2), opening up various possibilities to employ such LCPs in studies and applications of temperature-sensitive biological macromolecules.

To test the applicability of such low-temperature LCPs for the crystallization of membrane proteins, the light-induced proton pump bacteriorhodopsin (bR) was crystallized from MO- and MDS-LCPs at 20 °C in comparative experiments, as well as from MDS-LCP at 4 °C (see the Supporting Information). Plate-like hexagonal crystals with an average size of about  $18 \times 18 \times 7 \mu\text{m}^3$  were observed after three days in MDS at 20 °C, and grew to the full size (about  $40 \times 40 \times 20 \mu\text{m}^3$ ) in 10 days (Figure 4b). In contrast, crystallization in MO was slower, yielding fewer initial crystals (sized about  $20 \times 20 \times 7 \mu\text{m}^3$ ) under identical conditions after 10 days. These crystals grew to the full size in 28 days but remained smaller (about  $30 \times 30 \times 12 \mu\text{m}^3$ ) than in the MDS case. Moreover, using the same crystallization screen, crystals appeared in a much broader range of conditions in MDS than in MO. The best crystals observed at 4 °C were obtained from MDS after

28 days (Figure 4a). Crystals were subjected to X-ray crystallographic analyses using synchrotron radiation. They belonged to space group  $P6_3$ , with one protein molecule in the asymmetric unit. The best diffraction was obtained from crystals grown from MDS-LCP at 20 °C, and the structure was refined at 1.83 Å resolution (see Figures S4 and S5). The quality of the  $\sigma_A$ -weighted  $2mF_o - DF_c$  electron density map is shown in Figure 4c. BR crystals grown from MDS LCP at 4 °C were very small (about  $15 \times 15 \times 5 \mu\text{m}^3$ ), yet the crystal structure could be solved at 4.2 Å resolution (Figure S6), with identical unit cell parameters as those of the 20 °C-generated structure, confirming the validity of the approach at low temperature. Interestingly, the  $c$  axis in the MDS-grown crystals is unusually short (100 Å versus  $110 \pm 2$  Å in the MO-grown crystals). This may be due to the smaller thickness of the lipid bilayer formed by the geometrically confined and kinked MDS, resulting in a shorter  $c$  axis in the crystal, which is parallel to the transmembrane helices.

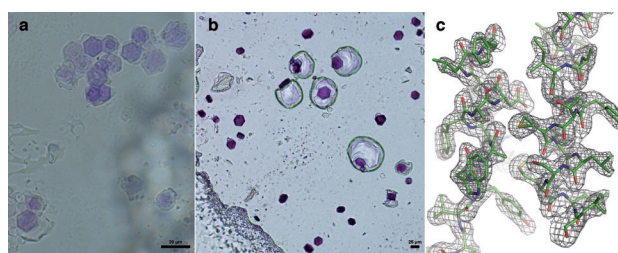


**Figure 4.** Comparison of bR crystals grown in MDS at a) 4 °C (20  $\mu\text{m}$  scale bar) and b) 20 °C (25  $\mu\text{m}$  scale bar). BR crystals in MDS constitute the first reported crystals of an integral membrane protein (IMP) grown at 4 °C from LCP. c) Quality of  $\sigma_A$ -weighted  $2mF_o - DF_c$  electron density map of bR crystallized in MDS at 20 °C, contoured at  $1.5\sigma$ .  $m$  = figure of merit;  $F_o$  = experimentally measured amplitudes;  $D = \sigma_A$  weighting factor;  $F_c$  (or  $F_{\text{model}}$ ) = model-based amplitudes.

In summary, we present here a designer lipid with which an important objective in membrane biophysics—establishing the relationship between lipid molecular structure and mesophase behavior—is addressed. A novel phase behavior is presented, with unprecedented features, which may be beneficial in various aspects and applications of membrane science and technology. Specifically, we have demonstrated the applicability of this novel LCP for membrane protein crystallization at unprecedented low temperatures.

### Experimental Section

Synthesis of 1-(*cis*-9,10-methylene-octadecanoyl)-*rac*-glycerol (compound 3 (MDS)): The synthesis of MDS was accomplished in two steps starting from commercially available oleic acid **1** (Figure S1). Cyclopropanation of olefin **1** was carried out with diethyl zinc and

diiodomethane in the presence of 2,4,6-trichlorophenol according to a method previously described in the literature<sup>[25]</sup> to afford *cis*-9,10-methyleneoctadecanoic acid **2** in 65% yield; which was then reacted with an excess of glycerol in the presence of EDC and 4-(dimethylamino)pyridine (DMAP) in dichloromethane to afford the desired ester **3** in 45% yield. The resulting racemic MDS is a mixture of the 1-MDS and 2-MDS isomers because of natural transesterification (Figure S2). The amount of the 2-MDS isomer was 6–10%, as determined by <sup>1</sup>H NMR spectroscopy. 1-MDS can be purified by low-temperature crystallization in acetonitrile (–20°C to 4°C). Prior to every sample preparation, the equilibrium state between the two isomers was established by stirring the synthesized lipid in a 5% aqueous solution of H<sub>2</sub>SO<sub>4</sub> for 3 h at room temperature; the composition was checked by <sup>1</sup>H NMR spectroscopy.

For detailed synthetic procedures see the Supporting Information.

**Mesophase sample preparation:** Liquid-crystalline mesophases were prepared by mixing weighed quantities of MDS and water (to the desired composition of each sample of the phase diagram) inside sealed Pyrex glass tubes followed by heating to 45°C and vortexing until a homogenous mixture was obtained. The prepared mesophases were then allowed to cool down to room temperature and reach a state of thermodynamic equilibrium over a period of 24 h before SAXS measurements were performed.

**Small-angle X-ray scattering measurements:** SAXS measurements were used to identify the symmetry of the mesophases at the different conditions. Experiments were performed on a MicroMax-002 + microfocused beam, operating at voltage and filament current of 45 kV and 0.88 mA, respectively. The Ni-filtered Cu K $\alpha$  radiation ( $\lambda$ Cu K $\alpha$  = 1.5418 Å) was collimated by three pinhole (0.4, 0.3 and 0.8 mm) collimators and the data were collected with a two-dimensional argon-filled Triton detector. An effective scattering-vector range of  $0.03 \text{ \AA}^{-1} < q < 0.45 \text{ \AA}^{-1}$  was probed, where  $q$  is the scattering wave vector defined as  $q = 4\pi \sin(\theta)/\lambda$  Cu K $\alpha$ , with a scattering angle of  $2\theta$ , calibrated using silver behenate. For all measurements the samples were placed inside a Linkam HFS91 stage, between two thin mica sheets and sealed by an O-ring, with a sample thickness of about 1 mm. Measurements were performed at different temperatures, and samples were equilibrated for 30 minutes prior to measurements, while scattered intensity was collected over 30 minutes. For the low-temperature experiments special care was taken to exclude supercooling.

Received: October 6, 2014

Published online: November 21, 2014

**Keywords:** lipid synthesis · membrane proteins · mesophases · phase behavior · small-angle X-ray scattering

[1] K. Larsson, *J. Phys. Chem.* **1989**, *93*, 7304–7314.

[2] L. C. Johansson, A. B. Wohri, G. Katona, S. Engstrom, R. Neutze, *Curr. Opin. Struct. Biol.* **2009**, *19*, 372–378.

[3] a) V. Cherezov, et al., *Science* **2007**, *318*, 1258–1265; b) A. Zabara, R. Negrini, O. Onaca-Fischer, R. Mezzenga, *Small* **2013**, *9*, 3602–3609; c) G. Katona, U. Andreasson, E. M. Landau, L. E. Andreasson, R. Neutze, *J. Mol. Biol.* **2003**, *331*, 681–692; d) V. I.

Gordeljiy, et al., *Nature* **2002**, *419*, 484–487; e) M. Kolbe, H. Besir, L. O. Essen, D. Oesterhelte, *Science* **2000**, *288*, 1390–1396; f) P. Nollert, *Methods* **2004**, *34*, 348–353.

- [4] a) J. C. Shah, Y. Sadhale, D. M. Chilukuri, *Adv. Drug Delivery Rev.* **2001**, *47*, 229–250; b) W. K. Fong, T. Hanley, B. J. Boyd, *J. Controlled Release* **2009**, *135*, 218–226; c) R. Negrini, R. Mezzenga, *Langmuir* **2011**, *27*, 5296–5303.
- [5] R. Mezzenga, P. Schurtenberger, A. Burbidge, M. Michel, *Nat. Mater.* **2005**, *4*, 729–740.
- [6] E. Nazaruk, E. Gorecka, R. Bilewicz, *J. Colloid Interface Sci.* **2012**, *385*, 130–136.
- [7] M. KomisarSKI, Y. M. Osornio, J. S. Siegel, E. M. Landau, *Chem. Eur. J.* **2013**, *19*, 1262–1267.
- [8] a) T. Landh, *FEBS Lett.* **1995**, *369*, 13–17; b) D. P. Siegel, *Biophys. J.* **1986**, *49*, 1171–1183.
- [9] Z. A. Almsheerqi, S. D. Kohlwein, Y. Deng, *J. Cell. Biol.* **2006**, *173*, 839–844.
- [10] a) E. M. Landau, J. P. Rosenbusch, *Proc. Natl. Acad. Sci. USA* **1996**, *93*, 14532–14535; b) V. Cherezov, *Curr. Opin. Struct. Biol.* **2011**, *21*, 559–566.
- [11] S. T. Hyde, *Curr. Opin. Solid State Mater. Sci.* **1996**, *1*, 653–662.
- [12] a) G. Lindblom, L. Rilfors, *Biochim. Biophys. Acta Rev. Biomembr.* **1989**, *988*, 221–256; b) V. Luzzati, H. Delacroix, A. Gulik, T. Gulik-Krzywicki, P. Mariani, R. Vargas, *Curr. Top. Membr.* **1997**, *44*, 3–24.
- [13] a) J. Briggs, H. Chung, M. Caffrey, *J. Phys. II* **1996**, *6*, 723–751; b) H. Qiu, M. Caffrey, *Biomaterials* **2000**, *21*, 223–234.
- [14] C. Fong, T. Le, C. J. Drummond, *Chem. Soc. Rev.* **2012**, *41*, 1297–1322.
- [15] D. F. Li, S. T. A. Shah, M. Caffrey, *Cryst. Growth Des.* **2013**, *13*, 2846–2857.
- [16] P. Eglhoff, M. Hillenbrand, C. Klenk, A. Batyuk, P. Heine, S. Balada, K. M. Schlinkmann, D. J. Scott, M. Schutz, A. Plückthun, *Proc. Natl. Acad. Sci. USA* **2014**, *111*, E655–E662.
- [17] S. H. White, W. C. Wimley, *Annu. Rev. Biophys. Biomol. Struct.* **1999**, *28*, 319–365.
- [18] U. Weierstall, et al., *Nat. Commun.* **2014**, *5*, 3309–3314.
- [19] a) B. Perly, I. C. P. Smith, H. C. Jarrell, *Biochemistry* **1985**, *24*, 4659–4665; b) E. J. Dufourc, I. C. P. Smith, H. C. Jarrell, *Chem. Phys. Lipids* **1983**, *33*, 153–177.
- [20] J. R. Silvius, R. N. Mcelhaney, *Chem. Phys. Lipids* **1979**, *25*, 125–134.
- [21] C. Sennoga, A. Heron, J. M. Seddon, R. H. Templer, B. Hankamer, *Acta Crystallogr. Sect. D* **2003**, *59*, 239–246.
- [22] V. Cherezov, J. Clogston, Y. Misquitta, W. Abdel-Gawad, M. Caffrey, *Biophys. J.* **2002**, *83*, 3393–3407.
- [23] a) D. L. Compton, K. E. Vermillion, J. A. Laszlo, *J. Am. Oil Chem. Soc.* **2007**, *84*, 343–348; b) S. Murgia, F. Caboi, M. Monduzzi, H. Ljusberg-Wahren, T. Nylander, *Prog. Colloid Polym. Sci.* **2002**, *120*, 41–46.
- [24] P. M. Duesing, R. H. Templer, J. M. Seddon, *Langmuir* **1997**, *13*, 351–359.
- [25] a) A. B. Charette, S. Francoeur, J. Martel, N. Wilb, *Angew. Chem. Int. Ed.* **2000**, *39*, 4539–4542; *Angew. Chem.* **2000**, *112*, 4713–4716; b) B. Jing, N. Tokutake, D. H. McCullough, S. L. Regen, *J. Am. Chem. Soc.* **2004**, *126*, 15344–15345.